

# GRADIENT ADAPTIVE IMAGE RESTORATION AND ENHANCEMENT

*Hongcheng Wang<sup>†</sup>, Yunqiang Chen<sup>‡</sup>, Tong Fang<sup>‡</sup>, Jason Tyan<sup>‡</sup>, Narendra Ahuja<sup>†</sup>*

<sup>†</sup>Beckman Institute, University of Illinois at Urbana-Champaign, Urbana, IL 61801

<sup>‡</sup>Intelligent Vision and Reasoning Dept., Siemens Corporate Research, Princeton, NJ 08536

## ABSTRACT

Various methods have been proposed for image enhancement and restoration. The main difficulty is how to enhance the structures uniformly while suppressing the noise without artifacts. In this paper, we tackle this problem in the gradient domain instead of the traditional intensity domain. By enhancing the gradient field, we can enhance the structure uniformly without overshooting at the boundary. Because the gradient field is very sensitive to noise, we apply an orientation-isotropy adaptive filter to the gradient field, suppressing the gradients in the noise regions while enhancing along the object boundaries. Thus we obtain a modulated gradient field, which is usually not integrable. We reconstruct the enhanced image from the modulated gradient field with least square errors by solving a Poisson equation. This method can enhance the object contrast uniformly, suppress the noise with no artifacts, and avoid setting stopping time as in PDE methods. Experiments on noisy images show the efficacy of our method.

## 1. INTRODUCTION

In many medical image processing applications, such as X-Rays, Ultrasound and MRI enhancement and restoration, noise needs to be suppressed while structure preserved or even enhanced. Signal processing based methods, such as wavelet [2], and more recently curvelet [10] and contourlet [1], have been efficiently used in image denoising since the noise is evenly distributed among the wavelet coefficients and is generally small. With a properly chosen threshold, the noise can be efficiently suppressed. On the other hand, signal-based methods, such as curvelet [11] and retinex enhancement algorithms [9], are also used for image enhancement. However, it is very hard for these methods to enhance edges consistently at different bandwidths. It usually overshoots at the edges but fails to bring out the contrast for the whole object.

Recently, some Partial Differential Equation (PDE) based methods have attracted much attention in image processing for their ability to reduce noise while preserving important features of the images. The linear isotropic diffusion equation is equivalent to Gaussian filtering, which may result in edge blurring or relocation. For nonlinear anisotropic diffusion such as Perona and Malik's formulation [6], the diffusion of image gray values depends on the gradient magnitude

and the diffusion is stopped across edges or discontinuities. However, it is very hard to determine the stopping time of diffusion to obtain nontrivial results. Coherence nonlinear anisotropic diffusion by Weickert [13] is more directional in both the gradient and the contour directions. This method may have "brushstroke" effects in non-structure regions due to the errors in local structure estimation.

In this paper, we propose a novel image restoration and enhancement method in the gradient domain. Intuitively, any drastic change in image intensity corresponds to large gradients, and any noise region corresponds to small or incoherent gradient field. The basic idea of this approach is to enhance the large gradient field and suppress the low gradient field, therefore enhancing the structure such as edges or discontinuities. High dynamic range image/video compression [4, 12] shares a similar flavor. Unfortunately, gradient domain method is usually very sensitive to high frequency noise, which is usually amplified by the gradient operator. Our scheme to deal with this problem is based on the local structure estimation. Our method can potentially avoid "overshooting" near the edges as in signal-based methods and has no "brushstroke" effect in the non-structure regions since it will not force structure onto a region that has none by direct suppression of the gradients of those regions.

The detail of our gradient-based image restoration method is explained in Section 2. In Section 3, we give some preliminary but very promising results. Finally, we draw the conclusion in Section 4.

## 2. GRADIENT-BASED IMAGE RESTORATION AND ENHANCEMENT

The main steps of the gradient-based image restoration and enhancement method are as follows: we first estimate the local structure properties (such as structure coherence and orientation) based on the gradient structure tensor. In the high structured region (corresponding to high coherence), the orientation-isotropy adaptive gaussian filter is applied to the gradient map, and then we enhance the large gradients. In the low structured or isotropic noise region (corresponding to low coherence), the gradient field is suppressed. Then, we can reconstruct a denoised image from the modulated gradient field. However, the modulated gradient field is usually not a valid

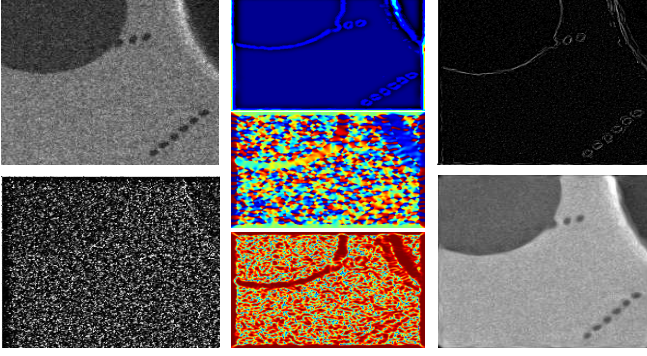


**Fig. 1.** Illustration of the algorithm. LEFT: noisy image (above) and its gradient (bottom); MIDDLE: structure coherence (above), orientation (middle) and isotropy (bottom); RIGHT: estimated gradient field (above) and reconstructed image (bottom) by solving a Poisson equation.

one since it will violate the zero-curl constraint, which will be explained in Section 2.3. By solving a poisson equation, we can then find the potential field (the filtered image) whose gradient field is closest to the modulated gradient field in the sense of least squares. These steps are illustrated in Figure 1.

## 2.1. Coherent Structure Analysis Using Gradient Structure Tensor

The structure tensor is defined as:  $T = \overline{\left(\frac{xx^T}{\|x\|^n}\right)}$ , where  $\overline{(\cdot)}$  indicates weighted local average. Structure tensor has been widely used in local coherence estimation. An efficient implementation of the structure tensor is the gradient structure tensor, which can be estimated in the following way. We first estimate the gradient  $g = \nabla I$  at scale  $\sigma_g$ , and then compute the gradients by convolving the image with the first order derivatives of a gaussian.

$$g_i = I(x) \otimes \frac{\partial}{\partial x_i} G(x; \sigma_g), i \in (1, \dots, N) \quad (1)$$

The gradient structure tensor is defined by  $T \equiv \overline{gg^T}$ .

In image processing, structure tensor is defined for a 2D neighborhood,  $I(x, y)$ , by:

$$T = \begin{bmatrix} I_{11} & I_{12} \\ I_{12} & I_{22} \end{bmatrix}, g = \begin{bmatrix} I_x \\ I_y \end{bmatrix} \quad (2)$$

where,  $I_{11} = \overline{I_x^2}$ ,  $I_{12} = \overline{I_x I_y}$ ,  $I_{22} = \overline{I_y^2}$ . We can then compute the eigenvalues of the matrix

$$\lambda_{1,2} = \left( I_{11} + I_{22} \pm \sqrt{(I_{11} - I_{22})^2 + 4I_{12}^2} \right) / 2 \quad (3)$$

with  $\lambda_1 \geq \lambda_2$ . The corresponding eigenvectors are determined by

$$v_1 \parallel v_2 = \left( \begin{array}{c} 2I_{12} \\ I_{22} - I_{11} + \sqrt{(I_{11} - I_{22})^2 + 4I_{12}^2} \end{array} \right) \quad (4)$$

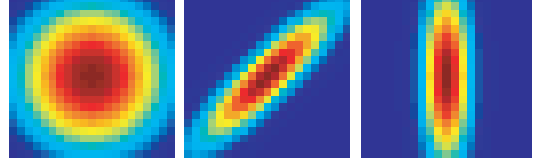


**Fig. 2.** Orientation-Isotropy Kernels. LEFT: Symmetric gaussian kernel with  $\sigma = 4$ ; MIDDLE: Kernel with  $\sigma_1 = 1, \sigma_2 = 4$  and  $\theta = \pi/4$ ; RIGHT: Kernel with  $\sigma_1 = 1, \sigma_2 = 4$  and  $\theta = \pi/2$ .

The eigenvectors,  $v_1$  and  $v_2$ , correspond to the directions of maximum and minimum variations, respectively.

Some properties can be obtained from the analysis of gradient structure tensor:

- *Confidence or Anisotropy,  $\alpha$* : Confidence measure is the confidence of structure orientation estimation, defined as  $\alpha = (\lambda_1 - \lambda_2) / (\lambda_1 + \lambda_2)$ . If  $\lambda_1 \approx \lambda_2$ , then  $\alpha \approx 0$ , and the structure is isotropic. If  $\lambda_1 \gg \lambda_2$ , then  $\alpha \approx 1$ , and the structure is linear or anisotropic.
- *Coherence,  $C$* : Local structure is estimated from  $\lambda_1$  and  $\lambda_2$ . Homogeneous regions are characterized by  $\lambda_1 = \lambda_2 \approx 0$ , edges by  $\lambda_1 \gg \lambda_2 \approx 0$  and corners by  $\lambda_1 \geq \lambda_2 \gg 0$ . Structure coherence measures the coherence within a window, defined by  $C = |\lambda_1 - \lambda_2| = \sqrt{(I_{11} - I_{22})^2 + 4I_{12}^2}$ .
- *Orientation,  $\theta$* : The second eigenvector of  $T$  defines the coherence orientation since it corresponds to the direction with the lowest fluctuations. The orientation is defined by  $\theta = \arctan(2I_{12} / (I_{22} - I_{11} + C))$ .

These parameters will be used for orientation-isotropy adaptive filtering in the following section.

## 2.2. Orientation-Isotropy Adaptive Filtering

In this section, we build an orientation-isotropy adaptive filter for image restoration and enhancement based on the structure coherence orientation and isotropy estimated above, similar to that by O'Malley and Kakadiaris [5]. However, we only estimate the filter kernel for the pixels whose coherence is larger than some threshold instead of for every pixel, since the regions with low coherence is usually noise region. We can directly suppress the gradient in those regions. Therefore, our method is more efficient. Secondly, the filtering in our method is operated on the gradient field, instead of on gray values of images, and thus we can obtain continuous surface in later image reconstruction process. For image enhancement, the new gradient field is obtained as follows:

$$g'_i = \begin{cases} \left( \frac{C}{\mu \cdot \text{Avg}(C)} \right)^p \cdot g_i, & \text{for } C \geq C_{thres} \quad (5) \\ \beta \cdot g_i, & \text{for } C < C_{thres} \quad (6) \end{cases}$$

where,  $\beta$  is the suppression factor ( $0 \leq \beta \leq 1$ ) for reducing the noise;  $Avg(C)$  is the mean value of the coherence in the structured regions;  $\mu$  ( $0 < \mu \leq 1$ ) and  $\rho$  ( $-1 \leq \rho < 0$ ) are constant. The parameters we used in practice are as follows:  $\mu = 0.3 \sim 0.6$ ,  $\rho = -0.2 \sim -0.4$ . It means that for the structured regions, we magnify the small gradient, where the coherence is smaller than  $\mu Avg(C)$ , and attenuate the large gradient such that the dynamic range of the image is compressed. Parameter  $\rho$  attenuates the gradient with larger coherence. For image restoration, the new gradient field is obtained as follows:

$$g'_i = \begin{cases} \gamma \cdot g_i \otimes G(\sigma_1, \sigma_2, \theta), & \text{for } C \geq C_{thres} \\ \beta \cdot g_i, & \text{for } C < C_{thres} \end{cases} \quad (7)$$

where,  $C_{thres}$  is the threshold value for coherence;  $\gamma$  is the enhancement factor, respectively ( $\gamma \geq 1$ ); and  $G(\sigma_1, \sigma_2, \theta)$  is the orientation-isotropy kernel with  $\sigma_1$  and  $\sigma_2$  defined by  $\sigma_1 = \sigma_{min} + (1 - \alpha)(\sigma_{iso} - \sigma_{min})$ ,  $\sigma_2 = \sigma_{iso}^2 / \sigma_1$ , where, the minimum scale for the minor axis,  $\sigma_{min}$ , is defined for preventing  $\sigma_2$  becoming zero. When  $\alpha = 0$ , we have the normal gaussian kernel with  $\sigma = \sigma_{iso}$ . Figure 2 illustrates some kernels with different orientation and isotropy.

### 2.3. Image Reconstruction From Gradient Field

Given a modified gradient field,  $G$ , our task is to reconstruct an image,  $I$ , whose gradient field is closest to  $G$ . One natural way to achieve this is to solve the equation  $\nabla I = G$ . However, since the original gradient field is modified, the resulting gradient field is not necessarily integrable. Some part of the modified gradient may violate  $\nabla \times G = 0$  (i.e. the curl of gradient is 0). In such a case, our task is to find a potential function  $I$ , whose gradients are closest to  $G$  in the sense of least squares by searching the space of all 2D potential functions, that is, to minimize the following integral in 2D space:

$$f = \min \iint F(\nabla I, G) dx dy \quad (9)$$

where,  $F(\nabla I, G) = \|\nabla I - G\|^2 = (\frac{\partial I}{\partial x} - G_x)^2 + (\frac{\partial I}{\partial y} - G_y)^2$ . According to the Variational Principle, a function  $F$  that minimizes the integral must satisfy the Euler-Lagrange equation:

$$\frac{\partial F}{\partial I} - \frac{d}{dx} \frac{\partial F}{\partial I_x} - \frac{d}{dy} \frac{\partial F}{\partial I_y} = 0 \quad (10)$$

We can then derive a 2D Poisson Equation:

$$\nabla^2 I = \nabla \bullet G \quad (11)$$

where  $\nabla^2$  is the Laplacian operator,  $\nabla^2 I = \frac{\partial^2 I}{\partial x^2} + \frac{\partial^2 I}{\partial y^2}$  and  $\nabla \bullet G$  is the divergence of the vector field  $G$ , defined as  $\nabla \bullet G = \frac{\partial G_x}{\partial x} + \frac{\partial G_y}{\partial y}$ .

In order to solve the Poisson equation (Equation 11), we use the Neumann boundary conditions  $\nabla I \cdot \vec{n} = 0$ , where

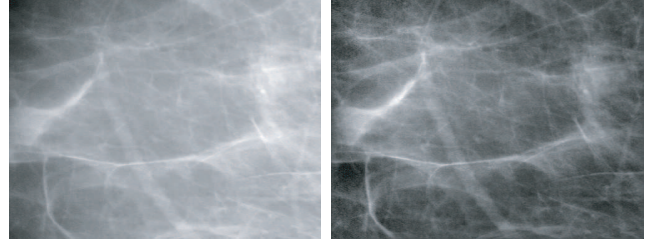


**Fig. 3.** Image Enhancement Results. LEFT: Original image; RIGHT: Enhanced image using our gradient-based method.

$\vec{n}$  is the normal on the boundary  $\Omega$ . In this case, the intensity gradients are approximated by forward difference:  $\nabla I = [I(x+1, y) - I(x, y), I(x, y+1) - I(x, y)]^T$ . We represent Laplacian as:

$$\nabla^2 I = [-4 \cdot I(x, y) + I(x-1, y) + I(x+1, y) + I(x, y+1) + I(x, y-1)].$$

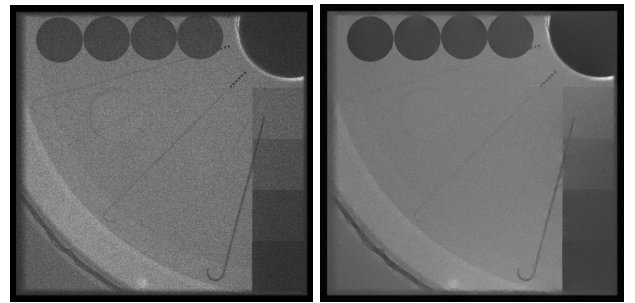
The divergence of gradient is approximated as:  $\nabla \bullet G = G_x(x, y) - G_x(x-1, y) + G_y(x, y) - G_y(x, y-1)$ .

This results in a large system of linear equations. We use the 2D multigrid algorithm [8] to iteratively find the optimal solution to minimize Equation 9.

### 3. EXPERIMENTAL RESULTS

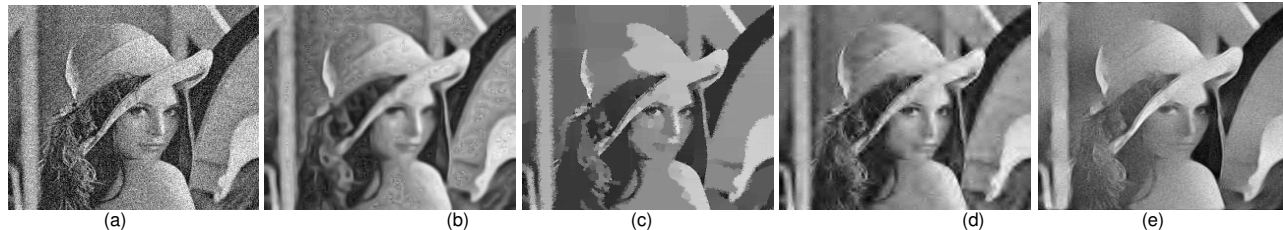
We give some examples in this section to illustrate the validity of our gradient-based algorithm in image enhancement and restoration.

Figure 3 is a noisy mammogram image with high intensity range (note the oversaturated bright region). Using Equations 5 and 6, we can efficiently enhance the structure of the image while suppressing some noise. The advantage of our algorithm for enhancement is that we can uniformly enhance the thin lines and the large objects. Most importantly, we do not have any overshooting problems. We experimentally chosen  $C_{thres} = 12$ .



**Fig. 4.** Image Restoration Results: (Left) Noisy image; (Right) Reconstructed image using our algorithm. (better viewed in PDF with magnification)

Figure 4 shows a denoising example of X-ray phantom with some thin structures. We can see that most of the structures in the image are preserved in our result. If the noise is



**Fig. 5.** Image Restoration Results Comparison Using Different Algorithms. (a) Noisy image; (b) Coherence enhancing diffusion; (c) Nonlinear diffusion; (d) Wavelet Denoising; (e) Reconstructed image using our gradient-based image restoration algorithm.

totally suppressed in the noise regions, the image will look unnatural for clinical practice. Therefore, we chosen  $\gamma = 1.5 \sim 2$  and  $\beta = 0.3$  in Equations 7 and 8. Other parameters we used in the experiment are:  $\sigma_{min} = 0.2$ ,  $\sigma_{iso} = 2$ , and experimentally chosen  $C_{thres} = 100$ . Figure 5 is the Lena image corrupted with zero-mean Gaussian noise (variance = 0.01). We can see that the image structures (edges and other discontinuities) are preserved and the noise is suppressed using our gradient-based method. Some structures on the face are missing. This is because our current implementation of the gradient computation is not optimized. We would like to apply multiple-scale technique to reliably detect all the significant intensity transitions in the future.

We compare our algorithm using the state-of-the-art image restoration algorithms: coherence enhancing diffusion, edge-preserving nonlinear diffusion, and wavelet-based method (we use the nonlinear diffusion package and wavelet package downloaded from Mathworks (<http://www.mathworks.com>). The "brushstroke" effect results in the noise regions using the coherence enhancing diffusion algorithm. For edge-preserving nonlinear diffusion, we carefully tuned the parameters (such as stopping time) for the best results. The filtered image in the left-bottom of Figure 5 has very flat regions, and some details are lost. The wavelet-based method has artifacts in sharp boundaries. Our gradient-based method preserves edges and suppresses noises at the same time. In the future, we would like to investigate the relationship between these methods and ours, and compare our method with most recent methods in image denoising [3, 7].

#### 4. CONCLUSION

We have described a novel image restoration and enhancement algorithm by combining the gradient domain method with the adaptive filtering method. We solve the intrinsic problem of the gradient domain method (e.g. sensitive to noise) and apply it to robustly enhance the structures and reduce the noise. Our method can enhance the structures uniformly without overshoot, suppress the noise with no artifacts, and avoid setting stopping time. We have obtained very promising image restoration and enhancement results using

the gradient-based method. We believe such a new approach will deliver a huge impact to the image processing society.

#### 5. REFERENCES

- [1] M. N. Do and M. Vetterli. The contourlet transform: an efficient directional multiresolution image representation. *IEEE Transaction on Image Processing*, to appear, 2004.
- [2] D. Donoho. De-noising by soft-thresholding. *IEEE Trans. Inform. Theory*, 41(3):613–627, 1995.
- [3] B. E.J., Y. Zheng, and R. Ewing. Feature-based wavelet shrinkage algorithm for image denoising. *IEEE Trans Image Process*, Dec.
- [4] R. Fattal, D. Lischinski, and M. Werman. Gradient domain high dynamic range compression. *ACM Transactions on Graphics (TOG)*, 21(3):249–256, July 2002.
- [5] S. O'Malley and I. Kakadiaris. Towards robust structure-based enhancement and horizon picking in 3-d seismic data. *IEEE Int. Conf. on Computer Vision and Pattern Recognition*, pages 482–489, July 2004.
- [6] P. Perona and J. Malik. Scale-space and edge-detection using anisotropic diffusion. *IEEE Transactions on Pattern Analysis and Machine Intelligence*, 12(7):629–639, 1990.
- [7] A. Pizurica and W. Philips. Estimating the probability of the presence of a signal of interest in multiresolution single- and multiband image denoising. *IEEE Trans Image Process*, Mar.
- [8] W. Press, S. Teukolsky, W. Vetterling, and B. Flannery. *Numerical recipes in C: the art of scientific computing*. Cambridge University Press, 1992.
- [9] Z. Rahman, D. J. Jobson, and G. A. Woodell. Retinex processing for automatic image enhancement. *Journal of Electronic Imaging*, 13(1):100–110, January 2004.
- [10] J.-L. Starck, E. J. Candès, and D. L. Donoho. The curvelet transform for image denoising. *IEEE Transactions on Image Processing*, 11(6):670–684, June 2002.
- [11] J.-L. Starck, F. Murtagh, E. J. Candès, and D. L. Donoho. Gray and color image contrast enhancement by the curvelet transform. *IEEE Transactions on Image Processing*, 12(6):706–717, June 2003.
- [12] H. Wang, R. Raskar, and N. Ahuja. High dynamic range video using split aperture camera. *IEEE 6th Workshop on Omnidirectional Vision, Camera Networks and Non-classical Cameras (OMNIVIS, in conjunction with ICCV'05)*, Oct. 2005.
- [13] J. Weickert. Coherence-enhancing diffusion of colour images. *Proc VII National Symposium on Pattern Recognition and Image Analysis*, 1:239–244, 1997.